MOLECULAR AND CELLULAR BIOLOGY, Nov. 2002, p. 7524–7534 Vol. 22, No. 21
0270-7306/02/$04.00+0 DOI: 10.1128/MCB.22.21.7524–7534.2002

High-Resolution Mapping of Changes in Histone-DNA Contacts of Nucleosomes Remodeled by ISW2

Stefan R. Kassabov,[1] Nathalia M. Henry,[1] Martin Zofall,[1] Toshio Tsukiyama,[2] and Blaine Bartholomew[1]*

Department of Biochemistry and Molecular Biology, Southern Illinois University School of Medicine, Carbondale, Illinois 62901-4413,[1] *and Division of Basic Sciences, Fred Hutchinson Cancer Research Center, Seattle, Washington 98109-1024*[2]

Received 4 June 2002/Returned for modification 16 July 2002/Accepted 6 August 2002

The imitation switch (ISWI) complex from yeast containing the Isw2 and Itc1 proteins was shown to preferentially slide mononucleosomes with as little as 23 bp of linker DNA from the end to the center of DNA. The contacts of unique residues in the histone fold regions of H4, H2B, and H2A with DNA were determined with base pair resolution before and after chromatin remodeling by a site-specific photochemical cross-linking approach. The path of DNA and the conformation of the histone octamer in the nucleosome remodeled or slid by ISW2 were not altered, because after adjustment for the new translational position, the DNA contacts at specific sites in the histone octamer had not been changed. Maintenance of the canonical nucleosome structure after sliding was also demonstrated by DNA photoaffinity labeling of histone proteins at specific sites within the DNA template. In addition, nucleosomal DNA does not become more accessible during ISW2 remodeling, as assayed by restriction endonuclease cutting. ISW2 was also shown to have the novel capability of counteracting transcriptional activators by sliding nucleosomes through Gal4-VP16 bound initially to linker DNA and displacing the activator from DNA.

The process of making DNA more or less accessible in eukaryotes plays a crucial role in the regulation of transcription, replication, recombination, and DNA repair. Several large multisubunit complexes reorganize chromatin in an ATP-dependent manner to either activate or repress these cellular processes (26, 44, 51, 53, 56, 57). ATP-dependent chromatin remodeling complexes contain an ATPase that has a well-conserved seven-domain region, and the ATPase activity is stimulated by DNA and nucleosomes (26). These chromatin remodeling complexes can be divided into four classes: the SWI/SNF and RSC, ISWI (for imitation SWI family), CHD/Mi-2, and INO80 families (12, 26, 28, 39, 43, 55). The ISWI protein in *Drosophila* is assembled into three distinct complexes (NURF, for nucleosome remodeling factor; CHRAC, for chromatin accessibility complex; and ACF, for ATP-utilizing chromatin assembly and remodeling factor), each with different subunit compositions and biochemical activities (9, 22, 23, 47, 49, 52). In yeast, there are two ISWI proteins, referred to as Isw1p and Isw2p, which are closely related by sequence to the *Drosophila* ISWI protein and are associated with one to three other polypeptides (48).

A general feature of the ISWI family of chromatin remodeling complexes is that they change the translational position of nucleosomes or slide nucleosomes (17, 20, 28, 29). In addition, all of the ISWI complexes except for NURF have been shown to help regularly space nucleosomes. The spacing activities of ISW1 and ISW2 differ in that ISW1 produces more regularly spaced arrays than ISW2, and the spacing varied from ~175 to ~200 bp for ISW1 and ISW2, respectively (48). ISWI, SWI/SNF, RSC, and Mi-2 have all recently been shown to induce torsional strain on DNA during remodeling (21). A distinguishing characteristic of these complexes is that ISWI requires histone tails for stimulation of its activity, whereas SWI/SNF and Mi-2 complexes do not (5, 6, 8, 15, 18). Furthermore, the ATPase activity of ISWI complexes is stimulated more by nucleosomes than free DNA, whereas the ATPase activities of SWI/SNF and RSC are equally stimulated by free DNA and nucleosomes.

Unlike SWI/SNF and RSC, which are both involved in transcription activation and repression, the in vivo function of ISW2 has been linked exclusively with repression. The SWI/SNF complex helps activate expression of the *INO1* gene in conjunction with Gcn5 containing histone acetyltransferase (HAT) complexes, whereas ISW2 acts with the histone deacetylase complex Sin3-Rpd3 to repress the gene (13, 16, 40). The repressive effect of ISW2 in this example is not dependent on the Sin3-Rpd3 activity, but is additive and presumably helps form a repressive chromatin structure independent of deacetylation of the histones. ISW2 and Sin3-Rpd3 are recruited through protein-protein interactions with the same repressor protein, Ume6, which binds to URS1 in the promoter region of *INO1*. A region within the *INO1*promoter was shown to become more inaccessible due to ISW2. ISW2 has also been shown to be required for the repression of several meiotic genes during mitotic growth (16). ISWI has been shown to be abundantly localized on the mitotic and polytene chromosomes, and its activity is required for the normal structure of the X chromosome, suggesting that ISWI has a global role in maintaining or establishing chromosomal structure (11).

An important question is what structural changes other than the translational position of the nucleosomes may be caused by ISW2 to create repressive chromatin. The biochemical characterization of nucleosomes remodeled by ISW2 has been carried out primarily by gel shift and nuclease accessibility assays, which are not well suited for differentiating structural changes in the remodeled nucleosome from changes in translational

* Corresponding author. Mailing address: Department of Biochemistry and Molecular Biology, Southern Illinois University School of Medicine, Carbondale, IL 62901-4413. Phone: (618) 453-6437. Fax: (618) 453-6440. E-mail: bbartholomew@siumed.edu.

positioning. For example, changes in the accessibility of DNA upon remodeling of nucleosomal arrays detected in earlier studies could have been the result of simple sliding of the nucleosomes to new positions, changes in the nucleosome structure, or both. The results of others employing mononucleosomes containing DNA with lengths of 146 or 155 bp showed no increase in DNA accessibility with ISWI-like proteins, which may arguably not be representative of the remodeled nucleosome, since no sliding of the nucleosome was observed (1, 29).

In this study, we have closely examined the structure of the ISW2 remodeled nucleosome, after sliding a short distance, by using a technique with base pair resolution to map contacts of three specific histone residues with DNA before and after remodeling. We have also tested the accessibility of nucleosomal DNA during the remodeling reaction and investigated the effect of binding of the transcription factor GAL4-VP16 to the linker DNA on nucleosome sliding by ISW2. We find that ISW2 efficiently slides nucleosomes positioned symmetrically near the ends of the183-bp DNA fragment to a single central position irrespective of the presence or absence of GAL4-VP16 binding. Importantly, the canonical spacing between the contacts of all modified histone residues on the DNA is strictly maintained after sliding, demonstrating a complete conservation of the nucleosome structure. Such maintenance of the canonical nucleosome structure together with the lack of enhancement of accessibility to an internal restriction endonuclease site during or after remodeling is in stark contrast with the disruptive remodeling carried out by members of the SWI/SNF-RSC family of complexes.

MATERIALS AND METHODS

Purification of ISW2 and Gal4-VP16. The ISW2 complex was purified from *Saccharomyces cerevisiae* strain YTT480, which contains two copies of the FLAG epitope added to the 3′ end of the *ISW2* gene. The ISW2 complex was affinity purified from the whole-cell extract by batch binding to anti-FLAG M2 agarose beads (Sigma) (10 μl of anti-FLAG M2 gel/ml of whole-cell extract) and gently eluted by competitive displacement with 2 mg of 3×FLAG peptide (Sigma) per ml in buffer A (25 mM Tris-HCl [pH 8], 0.5 mM EGTA, 0.1 mM EDTA, 2 mM $MgCl_2$, 20% glycerol, 0.02% Igepal) with 100 mM KCl.

Gal4-VP16 was overexpressed under the control of a *Tac* promoter with the pAC plasmid transformed into Xa-90 *Escherichia coli* cells (42). The cell lysate was precipitated by polyethyleneimine (PEI) and then by ammonium sulfate (45). The protein was loaded onto Q Sepharose and eluted with a linear gradient of 250 to 450 mM NaCl. The Gal4-VP16-containing fraction was further purified over a Mono S column with a linear gradient of 250 to 450 mM NaCl, and the protein was estimated to be 85 to 90% homogeneous.

Reconstitution of mononucleosomes. Mononucleosomes were assembled at 37°C by salt dilution with 12.6 μg of recombinant octamers, 160 fmol of ^{32}P-end-labeled DNA, 10 μg of sheared salmon sperm DNA, and 2.0 M NaCl in a starting volume of 10 μl (34). Salmon sperm DNA was sheared to a length of 100 to 700 bp by sonication. The sample was stepwise diluted to 1.2 M, 790 mM, and 300 mM NaCl, respectively, by addition of buffer B (25 mM Tris-HCl [pH 8.0], 1 mM 2-mercaptoethanol) at 10-min intervals. Nucleosome assemblies were analyzed on a 4% native polyacrylamide gel (acrylamide/bisacrylamide ratio, 38.9:1.1) in 0.5× Tris-borate-EDTA (TBE) at 4°C.

To obtain mononucleosomes of a homogenous length for ATPase assays, nucleosomes were reconstituted with 10 μg of PCR-amplified DNA and 12.6 μg of recombinant octamers. The DNA probes (183, 210, and 243 bp) for determination of the effect of linker DNA length on ISW2 activity were prepared by PCR amplification from the pGUB plasmid with Ampli*Taq* Gold polymerase (Applied Biosystems). The pGUB plasmid was constructed by inserting the 183-bp *Bam*HI fragment obtained from the pGALUSFBEND plasmid into the *Bam*HI site in pUC19 (24). In the PCRs, the same upstream primer (5′-CGGATCCTCTAGA CGGAG-3′) was used for all three DNAs, and the downstream primers were 5′-GATCCTCGATTCCATGGGGTACC-3′, 5′-GCTATGACCATGATTACG CCAAGCTTG-3′, and 5′-TTGTGAGCGGATAACAATTTC-3′ for the183-, 210-, and 243-bp DNAs, respectively. The assembly efficiency of nonlabeled nucleosomes was checked by 0.7% agarose gel electrophoresis and visualized with ethidium bromide as previously described (54).

Dyad axis and histone fold mapping. The histone H4 mutant, H4 S47C, was obtained from T. Richmond (14). H2A Ala45 and H2B Ser53 were replaced with cysteine by site-directed mutagenesis with the QuikChange kit from Stratagene. Reconstitution of nucleosomes with octamers that have one cysteine mutant histone and a complement of three other wild-type histones and 5′-end-labeled DNA was carried out as described above. Reaction mixtures containing nucleosomes with their respective unique cysteine (3.0 μM), 100 μM 2-mercaptoethanol, 25 mM Tris-HCl (pH 7.5), and 200 μM *p*-azidophenacyl bromide (APB; Fluka chemicals) in 1% dimethylformamide were incubated for 2 h at room temperature with 5% glycerol for selective coupling of the photoreactive group to the cysteine (7, 30, 38). The efficiency and selectivity of the reaction were monitored on a Triton-acid-urea (TAU) gel, in which the histone adduct's mobility is decreased with respect to unmodified histone. Excess APB was removed by dialysis, and modified nucleosomes were analyzed by gel shift assay.

Reaction mixtures containing the photoreactive nucleosomes were irradiated with a UV transilluminator at a setting of 310 nm for 1 min. A small portion of the irradiated reaction mixture was loaded onto a sodium dodecyl sulfate-polyacrylamide gel electrophoresis (SDS-PAGE) gel (17% polyacrylamide) to analyze the efficiency of cross-linking. SDS was added to a final concentration of 0.1%, heated at 70°C for 20 min, and extracted with phenol-chloroform (4:1). The organic phase and interphase were retained and washed three times with 1% SDS–1 M Tris-HCl (pH 8.0), and the sample was precipitated with ethanol.

The cross-linked DNA-protein complex was resuspended in 100 μl of 2% SDS, 20 mM ammonium acetate, and 0.1 mM Na-EDTA and heated for 20 min at 90°C. The reaction mixture was heated at 90°C for 45 min after the addition of 5 μl of 2 M NaOH. Alkaline cleavage was stopped by addition of 6.5 μl of 2 M HCl and an equal volume of 20 mM Tris-HCl (pH 8.0). The samples were ethanol precipitated, resuspended in 5 μl of formamide loading buffer (950 μl of deionized formamide, 25 μl of 2.5% bromophenol blue, 25 μl of 2.5% xylene cyanol), and analyzed on a 6.5% denaturing polyacrylamide gel along with a sequencing ladder of the same DNA obtained by a Sequenase quick denature procedure from U.S. Biochemicals. Final cut site assignments were made by comparing sequencing ladders with and without 5′ phosphorylation.

Synthesis of DNA photoaffinity probes. Single-stranded DNA was immobilized to streptavidin-coated Dynabeads (Dynal) as previously described (41), with the following changes for the synthesis of photoreactive 183-bp GUB DNAs. The pGUB DNA was cut with *Nde*I (NEB), after which biotinylated nucleotides were incorporated into the ends of the DNA by using the Klenow fill-in reaction. The biotinylated DNA was next cleaved with *Hin*dIII (NEB) to make a 404-bp biotinylated DNA containing the region to be modified. The 404-bp DNA was bound to streptavidin-Dynabeads M280, and the nonbiotinylated strand was removed from the beads by washing the beads under alkaline conditions. Primers 1 to 3 were annealed to template DNA for the synthesis of probes bp 12, 19, and 42. Probe bp 52/54 had primers 4 and 5 and probe bp 66 had primers 3 and 6 annealed to DNA and ligated with T4 DNA ligase. Photoreactive DB-dCMP was incorporated into probes bp 12, 19, 42, and 66, and DB-dUMP was incorporated into probe bp 52/54 by using the exonuclease-free Klenow fragment of DNA polymerase I (46). Immediately adjacent to the photoreactive nucleotide were incorporated [α-^{32}P]dGMP for probe bp 12, [α-^{32}P]dAMP for probes bp 19 and 44, or [α-^{32}P]dCMP for probes bp 52/54 and 66.

The oligonucleotide primers had the following sequences: primer 1, 5′-GGC CAGTGAATTCGGATCCTCTAGA-3′; primer 2, 5′-GGCCAGTGAATTCG GATCCTCTAGACGGAGGA-3′; primer 3, 5′-GGCCAGTGAATTCGGATC CTCTAGACGGAGGACAGTCCTCCGGTTACCTTCGAAC-3′; primer 4, 5′-GGCCAGTGAATTCGGATCCTCTAGACGGAGGACAGTCC-3′; primer 5, 5′-pTCCGGTTACCTTCGAACCACGTGGCCG-3′ ; and primer 6, 5′-pCACG TGGCCGTCTAGATGCTGACT-3′.

High-resolution gel shift analysis and photoaffinity labeling. In a standard 50-μl reaction mixture, ISW2 was incubated with nucleosome assemblies, with or without 300 μM ATP, at 30°C for 30 min under the following reaction conditions: 25 mM HEPES-KOH (pH 7.6), 5 mM $MgCl_2$, 0.1 mM EDTA, 10% glycerol, 50 mM KCl, and 0.1 μg of bovine serum albumin (BSA) per μl. For reactions in which Gal4-VP16 was included, 66.5 ng of Gal4-VP16 was incubated with nucleosome assemblies and ATP at 30°C for 30 min prior to the addition of ISW2. Of the 50-μl reaction mixture, 4 μl was analyzed by electrophoretic mobility shift assay on a 5% native polyacrylamide gel (acrylamide/bisacrylamide ratio, 60:1) in 0.2× TBE with buffer recirculation at 4°C. The remaining 46 μl of the sample was photocross-linked by UV irradiation for 5 min with a transilluminator (~310 nm). Chemical digestion of the DNA was carried out by the addition of 120 μl

of a 99% formic acid–2% diphenylamine solution (20 mg of diphenylamine in 1 ml of formic acid) at 70°C for 20 min to leave a small, uniform radiolabeled tag attached to the protein. Prior to digestion, 20 μg of octamer was added as a carrier, followed by the addition of 7 μl of a 20% lysine-cysteamine solution (200 mg of lysine, 200 mg of cysteamine in 1 ml of sterile water). Diphenylamine was removed by ethyl ether extraction (2×), and formic acid was removed by vacuum centrifugation. The cross-linked histones were precipitated with 10% trichloroacetic acid on ice for 30 min, pelleted by centrifugation at 20,000 × *g* (30 min, 4°C), and the pellet was washed twice with 100% acetone. After air drying, the pellet was resuspended in loading buffer (8 M urea, 0.9 N acetic acid, 10% glycerol, 5% 2-mercaptoethanol, 0.25% methyl green), heated at 90°C for 5 min, and loaded onto a 15% TAU gel (4). Prior to visualization of cross-linked histones by autoradiography, the gel was stained with Coomassie blue.

ATPase assay. An ATPase assay employing mononucleosomes assembled onto three lengths of pGUB DNA (183, 210, and 243 bp) was carried out as described previously (48), except that nucleosomes or free DNA was used at a final concentration of 100 nM with incubation at 30°C for 30 min. Unreacted ATP and free phosphate were separated by thin-layer chromatography by using PEI cellulose plates (Baker-Flex; J. T. Baker) with buffer E (0.8 M LiCl, 0.8 M acetic acid) as the solvent. Spots were quantified by phosphorimaging with a Cyclone Phosphorimager from Packard Instruments.

***Eco*RV accessibility assay.** Nucleosomes were assembled as described earlier and purified by sucrose density gradient sedimentation in a 5-ml gradient of 5 to 25% sucrose spun at 40,000 rpm (SW55 Ti rotor) for 14 h at 4°C. The purified nucleosomes (10 nM) were subjected to cleavage with *Eco*RV (200 U) in the presence of various amounts of ISW2 (2 to 150 nM) or SWI/SNF (50 nM) and ATP (800 μM) for 40 min at 30°C. Reactions were quenched with an equal volume of stop/loading buffer (1% SDS, 60 mM EDTA, 20 mM Tris [pH 7.5], 0.2% bromophenol blue) and deproteinized by incubation with 1 mg of proteinase K per ml for 1 h at 37°C. The cleaved DNA was resolved from the intact DNA on a 4% native polyacrylamide gel, and the signal in the bands was quantified by phosphorimaging.

RESULTS

The directionality of nucleosome sliding by ISW2. ISW2 slides nucleosomes to the center of DNA with mononucleosomes containing DNA of 210 and 243 bp as shown by gel shift assay, but no sliding was detected for nucleosomes with 183 bp of DNA (Fig. 1A, lanes 1, 8, and 15, respectively). Nucleosomes assembled on 210- and 243-bp DNAs have initially several translational positions with those positioned near the ends of DNA migrating the fastest (N1) and those near the center of DNA migrating the slowest (N4). Nucleosome sliding by ISW2 to the center requires the addition of ATP (compare lanes 5 and 8 with lanes 6 and 9). The lack of apparent nucleosome sliding of the183-bp nucleosome could be due to either the nucleosome having too short a linker DNA for ISW2 or the resolution of the gel shift assay not being adequate to observe small changes in translational position. The same directionality for nucleosome sliding has also been observed for the CHRAC complex from *Drosophila* (29).

Nucleosomal substrate requirement for the ATPase activity of ISW2. In order to determine if ISW2 was able to effectively bind the183-bp nucleosome, the ATPase activity of ISW2 was assayed with nucleosomes assembled on 183-, 210-, and 243-bp DNAs similar to those used in the sliding assay (Fig. 1B). The efficiency of nucleosome formation as assayed by gel shift for each DNA was comparable to that for all three DNAs at an overall efficiency of >85% (result not shown). The ATPase activity of ISW2 was stimulated by all three nucleosomal substrates to an equivalent amount and significantly over that without nucleosome or with free DNA. The same results were consistently obtained with different nucleosome reconstitutions, indicating that the183-bp nucleosome is as good a substrate for ISW2 as nucleosomes with longer DNAs.

High-resolution analysis of nucleosome sliding by ISW2. To better determine whether the183-bp nucleosome can be slid by ISW2, a technique was used to map the nucleosomal dyad axis with base pair resolution. The approach involved reconstitution of a recombinant histone octamer devoid of any cysteines, except for histone H4, which had serine 47 changed to cysteine (H4 S47C). The unique cysteines in the octamer were conjugated so as to place photoreactive aryl azides near DNA on either side of the dyad axis in the nucleosome (Fig. 2A). The mutant octamer was reconstituted onto the 183-bp DNA with one or the other DNA strands radiolabeled at its 5′ end (35). The extent of coupling of the aryl azide to mutant histone H4 in the nucleosome was shown to be quantitative by TAU gel analysis (result not shown). The photoreactive octamer was cross-linked to DNA, and the DNA was cleaved at the cross-linking site due to the instability of the DNA photoadduct formed.

In the upper and lower strands, four cleavage sites were detected in the samples containing nucleosome alone (Fig. 2B, lanes 1 and 4). The positions of the two cysteines in the nucleosome are separated by 8 bp of DNA. The cut sites at nucleotides 81, 89, 101, and 109 in the upper strand and at bp 79, 87, 100, and 107 in the lower strand correspond to cutting at two dyad axes at bp 84 and 104 (Fig. 2C). Each pair of cut sites was separated by 8 bp, and their position on the other strand was offset by 1 to 2 bp. The efficiencies of cutting at each pair of cut sites for the individual dyad axis were generally not equal, but there was a preference for cutting at the 5′ cut site, because of its closer proximity to DNA. This site preference is more readily seen with the dyad at bp 84, with more efficient cutting at nucleotide 82 than at nucleotide 90 in the upper strand and at both positions in the lower strand. These two translational positions are symmetrical with the nucleosome near either end of the DNA, showing slight differences in maximum linker DNA of 23 and 27 bp for positions A and B, respectively (Fig. 2C).

The changes in cut sites after addition of ISW2 and ATP show that the nucleosomes slide a short distance from either end toward the center of DNA (Fig. 2A, lanes 2 and 5). In the upper and lower strands, the cut sites corresponding to the dyads at bp 84 and 104 were lost, whereas new cut sites were observed that correspond to one major and one minor translational position (Fig. 2B, lanes 2 and 5). The cut sites at bp 90 and 98 in the upper strand and at bp 87 and 95/96 in the lower strand show that ISW2 slides the nucleosomes originally positioned near either end of DNA to principally a single centered translational position with its dyad at bp 93. The nucleosomes slid a total of 9 and 11 bp from their starting positions to the center. The minor altered nucleosome position is best seen in the upper strand, with two minor cut sites at bp 86 and 94 that map a subpopulation of nucleosomes located between the new dyad at bp 93 and the original dyad at bp 84. These results show that ISW2 can slide nucleosomes with as little as 23 bp of linker DNA, and the nucleosomes are preferentially slid to the most central position, similar to that observed with longer DNAs.

Evidence for maintenance of the canonical nucleosome structure after sliding by ISW2. Changes in histone-DNA contacts in the regions of the histone fold of H2A/H2B after remodeling were examined by photoreactive histone octamers. Histone octamers were made in which the only cysteine in the

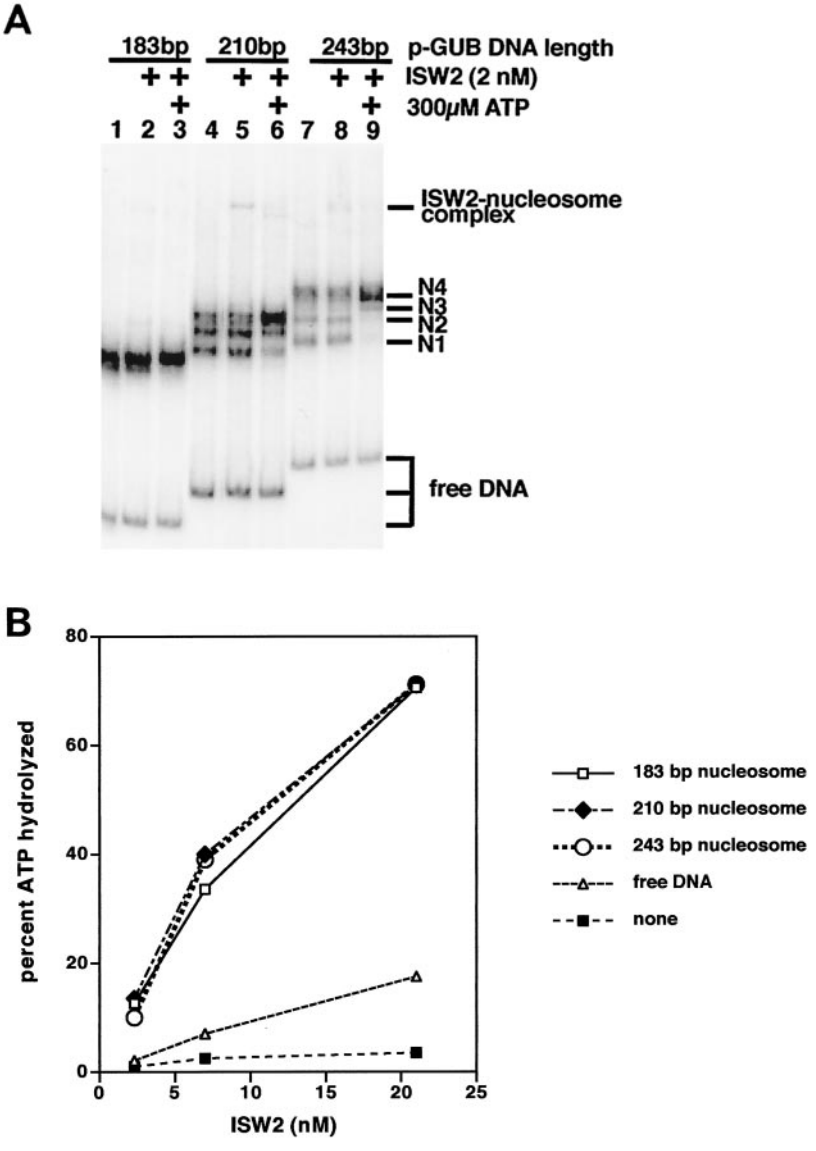

FIG. 1. Evidence for sliding of mononucleosomes to the center of DNA by ISW2. (A) Nucleosomes were reconstituted on radiolabeled DNAs of 183, 210, and 243 bp and separated on a native 5% polyacrylamide gel. The longer DNAs when assembled into nucleosomes bound in different translational positions that were resolved and are indicated as N1 to N4 on the right. ISW2 and ATP were added as indicated at the top of the lanes. (B) The ATPase activity of ISW2 is stimulated by nucleosomes with as little as 183 bp of DNA. Mononucleosomes were reconstituted with recombinant histone octamer and DNAs of 183, 210, and 243 bp and used as substrate in ATPase assays of ISW2. Three different concentrations of ISW2 were used: 21, 7, and 2.3 nM.

octamer was in either histone H2A (Ala 45 changed to Cys) or H2B (Ser 53 to Cys) to map the DNA sites close to these two residues before and after ISW2 remodeling. These amino acid residues are at the junction between loop 1 and alpha helix 2 of the H2A/H2B histone fold, close to the two main contact points of this histone fold with DNA. Nucleosomes containing these mutant octamers were modified as described before so that a photoreactive aryl azide was coupled to cysteine. Modified Cys 53 of H2B cross-linked and cut DNA at bp 30, and modified Cys 45 of H2A cross-linked and cut DNA at bp 123 in the upper strand (Fig. 3A, lanes 1 and 5). On the lower strand, the strongest cross-link with H2B was at bp 138, and the strongest cross-link with H2A was at bp 45 (lanes 8 and 12). Residue 45 of H2A and residue 53 of H2B are located 39 and 54 bp, respectively, from the dyad axis in the nucleosome crystal structure, which precisely correlates with the H2A and H2B cut sites on both strands for the dyad axis at bp 84 (Fig. 3B). Although there are two modifications per nucleosome, only one cleavage site per DNA strand was observed for either the modified H2A or H2B, indicating that the residues are proximal to only one of the two strands at each site. In other experiments, cutting at bp 108 in the lower strand with modified H2B was shown to be from small amounts of subnucleosomal particles (lane 8) (results not shown).

The exceptionally good correlation of the distance between DNA cut sites from residue 47 of H4, to 45 of H2A, to 53 from H2B with the crystal structure demonstrates that the cysteine replacements and covalent attachment of aryl azide to those

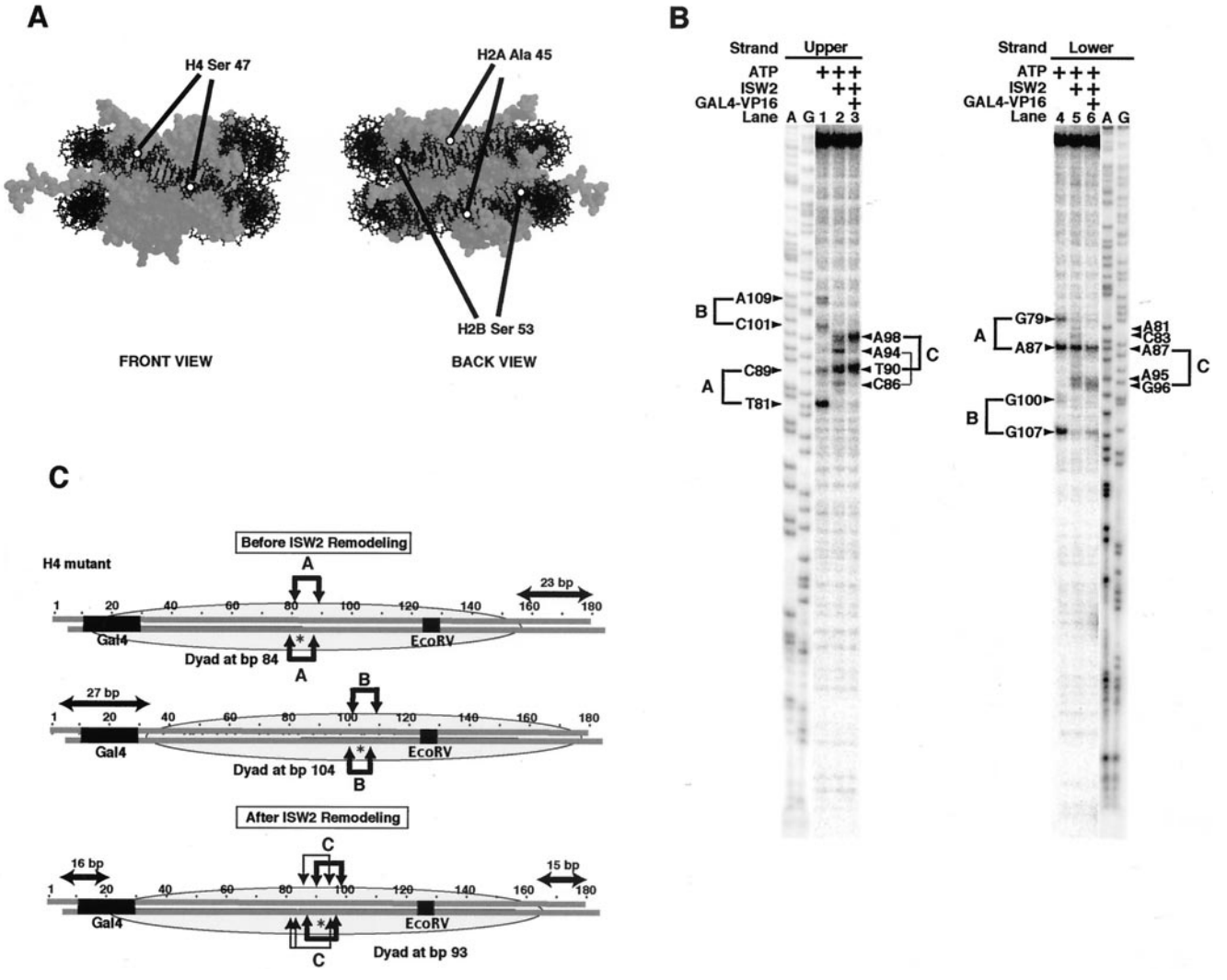

FIG. 2. High-resolution mapping of the 183-bp nucleosome before and after ISW2 remodeling. (A) The locations of the site-specific modification of the nucleosome at histone H4 residue 47, histone H2A residue 45, and histone H2B residue 53 are shown on the nucleosome. The nucleosome structure is shown with the specific residues highlighted by open circles and with the nucleosome shown in two orientations rotated 180° around the DNA superhelical axis (front and back views). (B) Site-directed mapping results with histone octamers containing histone H4 with Cys 47 coupled to an aryl azide. DNA radiolabeled at the 5′ end of either the upper or lower strand was used to map the location of the DNA cleavage site induced by the cross-linking of histone H4. The A and G sequencing ladders of the same DNA with unphosphorylated primers (labeled A and G) were also loaded for comparison. A lighter exposure of the sequencing ladders is shown to compensate for the higher level of signal in these lanes. The samples contained ATP (300 μM), ISW2 (2 nM), and Gal4-VP16 (50 nM), as indicated at the top of each lane. (C) Cut sites on the upper and lower strands of the 183-bp DNA are shown by arrows above and below the DNA sequence. The cut sites corresponding to each translational position, referred to as A, B, and C, are shown separately. The asterisk indicates the dyad axis of each, as mapped by the DNA cut sites, and the position of the nucleosome is shown as a shaded oval over the DNA sequence. The thickness of the arrow represents the relative efficiency of cutting, and the *Eco*RV restriction endonuclease site is underlined in the DNA sequence and labeled.

residues did not affect the structure or the translational position of the nucleosome. The modified H2A and H2B octamers did not show as much of the nucleosomes at the dyad at bp 104 as did the H4 mutant octamers. The relative amounts of nucleosomes positioned at the dyad at bp 84 and 104 may be affected by subtle changes in assembly conditions. Although not as abundant, nucleosomes were detected at the dyad at bp 104 with cutting at bp 158 for H2B and bp 65 for H2A on the lower strand and at bp 50 for H2B and bp 138 to 143 for H2A on the upper strand (Fig. 3A, lanes 1, 5, 8, and 12, and Fig. 3B).

After ISW2 remodeling, the H2A and H2B contacts with DNA were moved 8 to 12 bp from their starting position to a more central position correlating well with the dyad axis being repositioned (Fig. 3A and B). H2B contacts on the upper strand were moved from bp 30 to 39 (Fig. 3A, compare lanes 1 and 3), and those on the lower strand were moved from bp 138 and 158 to bp 146 and 148 (compare lanes 8 and 10). H2A contacts changed in a similar manner from bp 123 to 131 in the upper strand (compare lanes 5 and 6) and from bp 45 and 65 to 53 in the lower strand (compare lanes 12 and 13). The changes in H2A and H2B contacts with DNA caused by ISW2 correspond precisely to the change in the dyad axis determined with the H4 mutant octamer (Fig. 3B). The conservation of the same DNA spacing between the H2A, H2B, and H4 sites near

the dyad axis and in either direction from the dyad axis shows that the path of DNA on the nucleosome is likewise conserved after being slid by ISW2.

A minor new cut site was generated after ISW2 remodeling at bp 133 on the lower strand with modified H2A (Fig. 3A lane 13). Cutting at bp 133 is most likely caused by a loss of the strict cross-linking preference for the upper strand at bp 131 to cross-linking of both DNA strands from the same site on the histone octamer. The loss of strand specificity probably indicates that the DNA on the surface of the remodeled nucleosome is slightly twisted, bringing the second DNA strand in closer proximity to H2A modified at residue 45. A similar cut was not observed on the other side of the dyad on the upper strand near bp 53. The loss of strand specificity on one side of the dyad and not the other could be due to slight differences in DNA twist caused by differences in the DNA sequence. Similar differences have also been observed in the nucleosome crystal structure (33). No loss of strand specificity was observed with modified H2B, which is not surprising, since the position of the two DNA strands with respect to H2B residue 53 is very inflexible due to a nearby arginine protruding through the minor groove of DNA.

DNA photoaffinity labeling was also used to probe changes in histone-DNA contacts after ISW2 remodeling. Histone-DNA interactions were probed primarily in a region from bp 12 to 66. Photoreactive nucleotides were incorporated into the 183-bp DNA fragment at single, specific nucleotide positions, and adjacent to these, radioactively labeled nucleotides were incorporated for DNA photoaffinity labeling of histones bound near these sites (Fig. 4A). After assembly of the nucleosome with the photoreactive DNA templates and incubation with and without ISW2 and ATP, the complexes were photocross-linked by UV irradiation.

Several changes in histone-DNA interactions were detected at five different positions in DNA due to ISW2 remodeling and are consistent with sliding of the nucleosome by 8 to 12 bp with retention of the canonical nucleosome structure. DNA photocross-linking at bp 12 near the edge of nucleosomes with their dyad at bp 84 provides evidence for the movement of the histone octamer away from the edge of the DNA by ISW2 (Fig. 4B, lanes 1 to 4). Histone H2A is cross-linked most efficiently at this position (lanes 1 and 2), and upon ISW2 remodeling, labeling of H2A is greatly reduced, with no other histones becoming cross-linked (lane 3). While cross-linking of H2A is reduced by ISW2 and ATP at bp 12, only 7 bp away at bp 19, there is an increase in H2A cross-linking that is dependent on ISW2 and hydrolysis of the gamma phosphate of ATP (compare lane 7 with lanes 6 and 8). Histone H3 was cross-linked at bp 19 both before and after ISW2 remodeling. The close proximity of H3 to DNA in the original nucleosome is expected, as can be seen in the crystal structure of the nucleosome at the equivalent position. After sliding the nucleosome, bp 19 is moved to just outside of the 146 bp of core DNA based on the previous mapping data. Although not depicted in the crystal structure, it can be readily seen how both H2A and H3 might be in close proximity to this site in the DNA slightly outside of the core particle.

A similar change in histone cross-linking was observed at bp 42 and 52/54, with a loss of H2A cross-linking at bp 42 and a gain of H2A cross-linking at bp 52/54 after ISW2 remodeling (lanes 9, 11, 13, and 15). H2A cross-linking at bp 42 is most likely due primarily to nucleosomes at the dyad at bp 84 and would cross-link near the region of H2A that was modified in the previous mapping procedure at amino acid 45. Along with the loss of H2A cross-linking at bp 42 after addition of ISW2 and ATP, there is also a significant increase in H2B cross-linking due to ISW2 (lane 11). Base pair 42 is 59 nucleotides away from the new dyad axis formed by ISW2 sliding of the nucleosome, and as expected from the crystal structure, it would be close to H2B. After sliding the nucleosome to a dyad axis at bp 93, it would be expected based on the crystal structure that H2A and H2B would both be in close proximity to DNA 47 to 49 bp away from the dyad axis at bp 52/54.

At bp 66, there are two noticeable changes that occur upon addition of ISW2 and ATP (i.e., the reduction of histone H2A and increase of H4 cross-linking [lanes 17 and 19]). It appears that most of the cross-linking at this position is not from the dyad at bp 84, which would be H3 and H4, but instead is from the dyad at bp 104 with efficiently cross-linked histone H2A. The position of the probe with the dyad at bp 84 is not optimal for cross-linking of histone H3 and H4. The increase in H4 cross-linking observed after ISW2 remodeling is consistent with the new dyad axis being located ~24 bp away and thus positioning H4 close to DNA. The changes observed in H2A, H2B, and H4 cross-linking at five DNA positions are all consistent with the previous site-directed histone mapping data showing sliding of the nucleosome from the ends of DNA toward the center with no change in the canonical nucleosome structure.

Gal4-VP16 binding does not interfere with nucleosome sliding by ISW2. The 183-bp DNA contains a Gal4 binding site inside of the nucleosome-bound region or in the linker region, depending on the translational position (Fig. 2C, positions A and B). It has been proposed that ISWI binds to linker DNA and pushes the DNA in toward the nucleosome to slide the nucleosome (27). Gal4-VP16 binding to most of the 27 bp of linker DNA with the dyad at bp 104 could interfere with ISW2 binding to linker DNA and act as a barrier to prevent sliding toward the Gal4 site. The position of the altered nucleosome was mapped with base pair resolution as before, except in this case, Gal4-VP16 was quantitatively bound to the nucleosome before addition of ISW2 and ATP and assayed by gel shift (Fig. 3C) (data not shown). Nucleosomes were efficiently slid from both translational positions, as shown by site-directed mapping with the modified histones. The dyad positions were slightly more efficiently changed to the new dyad axis with the addition of Gal4-VP16, as seen by the elimination of the minor translational position with loss of cutting at bp 94 and 86 in the upper strand (Fig. 2B, compare lanes 2 and 3) and bp 81, 83, and 95 in the lower strand (compare lanes 5 and 6). Similar mapping results were obtained with modified H2B and H2A, in which no change in the extent or position of nucleosome sliding to the center was observed due to the Gal4-VP16 binding to the linker DNA (Fig. 3A, compare lanes 3, 7, 11, and 14 to lanes 2, 6, 10, and 13). Sliding from the dyad at bp 104 to the new dyad at bp 93 would push the edge of the nucleosome midway through the Gal4 site and thus suggest that Gal4-VP16 does not present a significant block to nucleosome sliding by ISW2. Gal4-VP16 remains bound to the nucleosome even after sliding the nucleosome over half of its binding site, as evident by gel shifting (Fig. 3C, compare lanes 2 and 4). Gal4-VP16 binding alone to the nucleosome did not cause the nucleosome to change its translational position or even its contact imme-

diately adjacent to the Gal4 site (Fig. 3A, compare lanes 2 and 9 with lanes 1 and 8) (data not shown with H4). The fact that there is no interference with nucleosome sliding by Gal4-VP16 suggests that either ISW2 does not need to bind to the linker DNA, or Gal4 and ISW2 may be able to simultaneously bind to the linker DNA.

A strong nucleosome positioning sequence was used to place the nucleosome at one end of a 281-bp DNA fragment immediately adjacent to a Gal4 site to determine if the nucleosome can be slid more completely through the Gal4-bound site (32). After sliding of the nucleosome by ISW2 to the center of the 281-bp DNA, the Gal4 site would be located near the dyad axis of the nucleosome. In the absence of Gal4-VP16, nucleosomes were slid to the center and to intermediate positions on the DNA after incubation with ISW2 and ATP (Fig. 5, compare lanes 4 to 6 to lane 1). Quantitative binding of Gal4-VP16 to the nucleosomes was achieved (lane 2), and then ISW2 and ATP were added to the Gal4-nucleosome complex and incubated for 1 to 15 min (lanes 7 to 10). In order to assess the extent of sliding in the presence of Gal4-VP16 bound to the nucleosome, the reaction was stopped with competitor DNA and γ-S-ATP, and Gal4-VP16 was released with Gal4-specific competitor DNA (lanes 11 to 13). The Gal4-VP16 bound to DNA did not present a significant barrier to nucleosome sliding by ISW2, as seen by the nucleosomes being slid to nearly the same extent in the presence or absence of Gal4-VP16 (compare lanes 4 to 6 to lanes 11 to 13). The rate of nucleosome sliding is somewhat slower in the presence of Gal4-VP16, as evident by having nearly twice as much of the nucleosomes remaining in their original position after 15 min compared to those without Gal4-VP16. Gal4-VP16 is also displaced by ISW2 sliding nucleosomes through its site as the amount of the Gal4-nucleosome complex decreased over the time of sliding (compare lane 9 to lanes 7 and 8). Nucleosomes that have slid toward the center have Gal4-VP16 preferentially released, as can be seen by comparing the free nucleosomes present before and after competition of Gal4-VP16 with unlabeled Gal4 competitor DNA. In lanes 8 and 9, less of the free original nucleosome is evident without the addition of the Gal4 competitor than in lanes 12 and 13, whereas, free nucleosomes that have slid toward the center are equally present with or without the Gal4 competitor.

ISW2 does not disrupt the nucleosome. Next, it was important to determine if ISW2 could at any time during its remodeling reaction cause the nucleosomal DNA to become more accessible, as has been observed for other ATP-dependent chromatin remodeling complexes. Earlier studies were either conducted with nucleosomal arrays in which changes in accessibility could be caused by changes in translational position and not in the core nucleosome structure or with mononucleosome assembled on DNAs too short to allow sliding (1, 29, 48). In contrast, the 183-bp nucleosome used in this study is well suited for examining DNA accessibility due to the process of nucleosome sliding and not merely to the new translational positions leaving the site exposed in the linker region. Accessibility of nucleosomal DNA was probed by restriction endonuclease cutting assays with *Eco*RV. The *Eco*RV restriction cut site at bp 124 to 129 is located within the nucleosome-bound region of DNA of both starting translational positions and that of the remodeled nucleosome. The restriction endonuclease *Eco*RV was added with ISW2 and ATP and incubated for 30 min so that transient or more stable changes causing increased access to nucleosomal DNA could be detected (Fig. 6). The small amount of DNA cut in the nucleosome alone sample corresponds to the small amount of DNA not packaged into the nucleosome (lane 1). No significant increase in nuclease cutting was observed at ISW2 concentrations ranging from 2 to 150 nM in the presence of ATP (lanes 3 to 7). The largest amount of ISW2 used in these experiments is in large excess of the amount of protein required to observe efficient and complete sliding of the nucleosome. In contrast, the yeast SWI/SNF complex was able to efficiently disrupt the nucleosome, as is evident by an increase in efficiency of *Eco*RV cleavage from 8 to 89% (lane 2). Although ISW2 slides the nucleosome about one helical turn of DNA, no formation of DNA loops or other conformational changes that would cause enhanced cutting by *Eco*RV could be detected.

DISCUSSION

In this study, the ISW2 chromatin remodeling complex was shown to preferentially slide nucleosomes to the center of DNA without changing the path of DNA or the histone octamer conformation in the slid nucleosome. Nucleosome sliding by ISW2 was shown to be from the ends toward the center of DNA by changes in electrophoretic mobility of nucleosomes containing 210- and 243-bp DNAs and by a photochemical method that affords high-resolution mapping of histone-DNA contacts in 183-bp nucleosomes. The structure of the remodeled nucleosome was examined by determining where six specific sites of the H2A/H2B and H3/H4 histone folds contact DNA before and after ISW2 remodeling. The site-specific cleavage of DNA in the region of the H3/H4 histone fold surrounding the dyad axis revealed that nucleosomes were efficiently slid with as little as 23 bp of linker DNA by ISW2 from two major translational frames near either end of the 183-bp DNA to one new primary translational position at the center of the DNA. The other modification sites in the histone octamer were designed to complement those at the dyad axis and were targeted 39 and 54 bp in both directions from the dyad axis. Preservation of the canonical nucleosome structure after nucleosome remodeling and sliding by ISW2 was shown by the six octamer sites remaining proximal to DNA and the spacing between these sites being strictly conserved. Mapping the histone-DNA contacts and the distance on DNA between the six histone sites is a sensitive assay for changes in nucleosome conformation, since distortions of the path of DNA due to either over- or underwinding, creation of short loops off the surface of the octamer, or other changes in the nucleosome structure would perturb these contacts. DNA photoaffinity labeling data also support the conclusion drawn from the site-directed histone mapping by determining which histones are close to different DNA sites.

Restriction endonuclease cutting assays showed that there was no increased accessibility of nucleosomal DNA due to the quantitative sliding of the nucleosome by ISW2. Previous studies showed that the recombinant human ISWI (Snf2H) and CHRAC do not make nucleosomal DNA more accessible, but in contrast to this study, the nucleosomes were not shown to have been slid (1, 29). In these studies, the nucleosomes were unlikely to have been slid, because of the absence or lack of sufficient linker DNA. ISWI complexes have been shown to enhance accessibility of DNA to restriction endonuclease cutting by nucleosomal arrays (48). In these cases, it was not

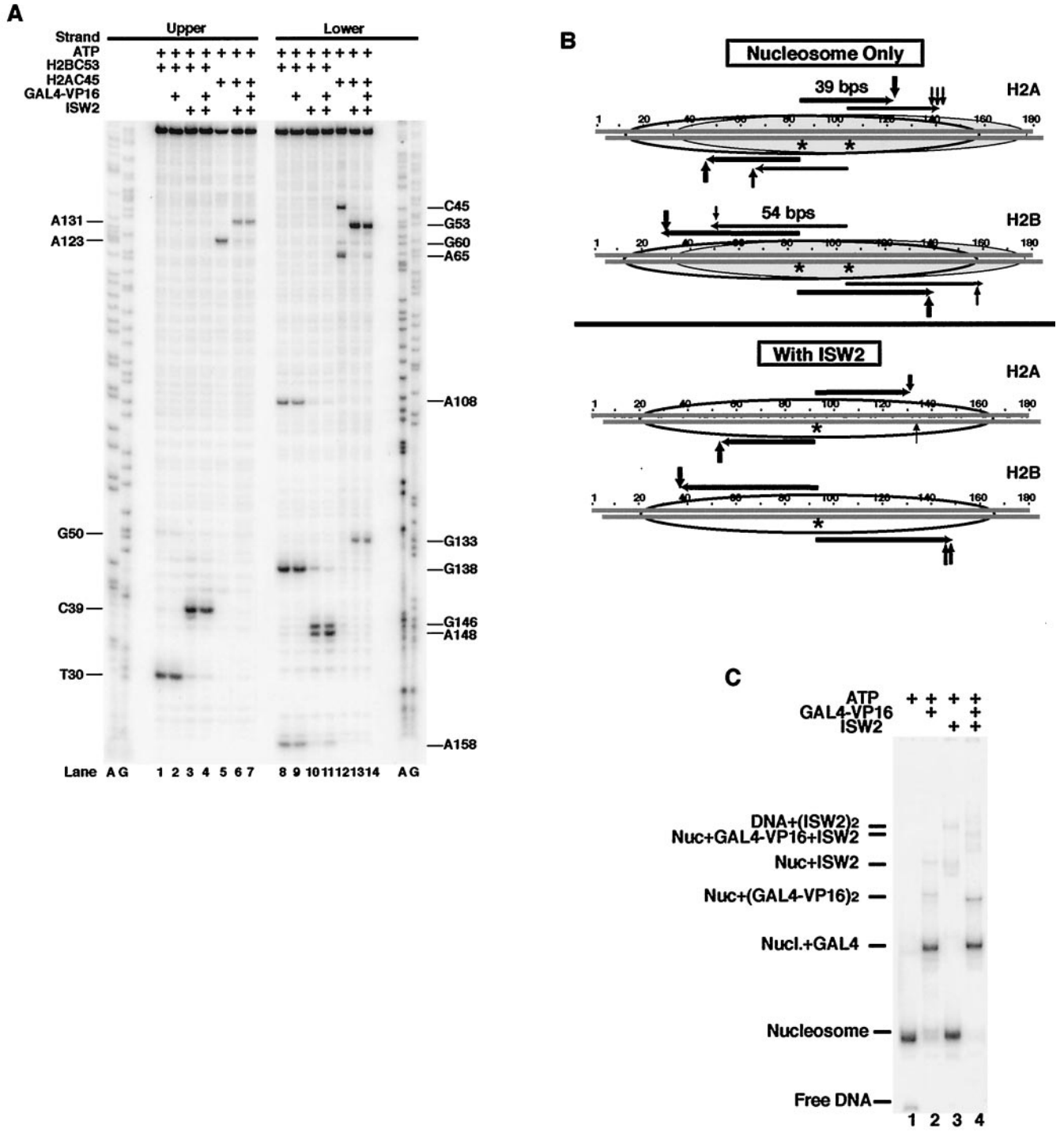

FIG. 3. Mapping the changes in the position of the H2A/H2B histone fold with DNA before and after ISW2 remodeling. (A) DNA mapping results with histone octamers containing mutant H2A Ala 45 or H2B Ser 53 changed to Cys are shown. Samples were prepared and processed as described in the legend to Fig. 2B. The locations of the cut sites are indicated on the left and right sides. The modified histone octamer used in each sample is indicated at the top of the lane. ISW2, Gal4-VP16, and ATP were added as indicated. (B) Summary of the DNA cleavage results with histone octamers modified at residues 45 of H2A and 53 of H2B with correlation to the dyad axis mapping results for histone octamers modified at residue 47 of H4. The vertical arrows above and below the DNA sequence indicate the cut sites obtained with modified H2A or H2B. The horizontal arrows show where the predicted cut sites would be based on the previously determined dyad axis for either the unremodeled or remodeled nucleosome. (C) Gal4-VP16 is bound quantitatively to the183-bp nucleosome before and after remodeling. Small portions of the H2B C53 mapping reactions analyzed in panel A, lanes 1 to 4, were loaded onto a 4% native polyacrylamide gel to assess the extent of Gal4-VP16 and ISW2 binding to the nucleosome. Identical results were obtained with the other two modified nucleosomes (data not shown).

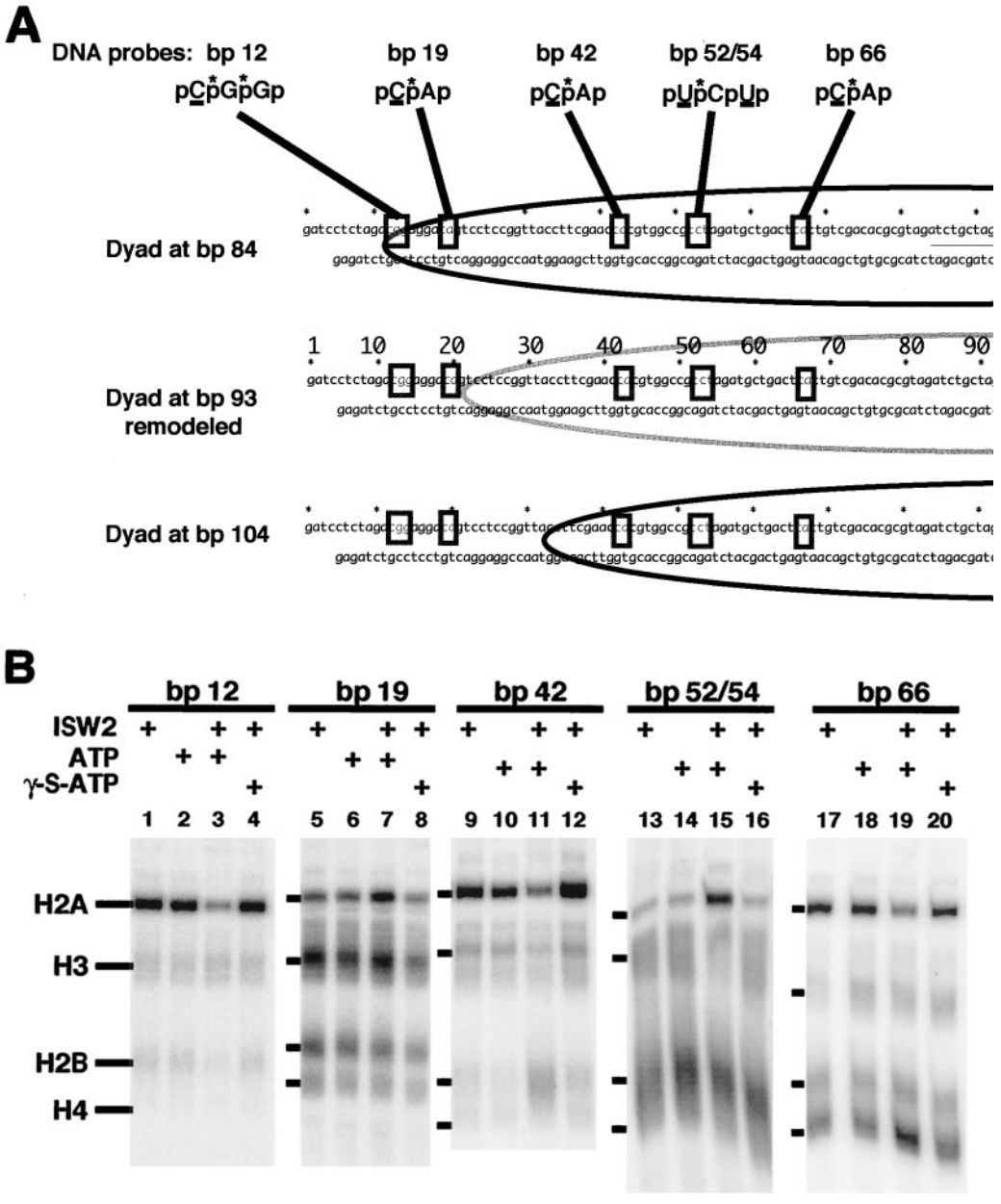

FIG. 4. DNA photoaffinity labeling of histones from bp 12 to 66. (A) Five DNA photoaffinity probes were constructed from the 183-bp GUB DNA with photoreactive and ^{32}P-labeled nucleotides incorporated at the depicted sites. The underlined C and U are the photoreactive nucleotides DB-dCMP and DB-dUMP, and the asterisk over the p is the ^{32}P-labeled phosphodiester. The relative positions of these modifications in the nucleosome are shown before (dyads at bp 84 and 104) and after (dyad at bp 93) ISW2 remodeling. (B) The nucleosomes were assembled with 183-bp modified DNA probes containing photoreactive nucleotides at bp 12, 19, 42, 52/54, and 66 in the top strand. ISW2, ATP, and γ-S-ATP were added as indicated above each lane. The photoaffinity-labeled samples were processed as described in Materials and Methods and visualized by phosphorimaging.

possible to determine if the increase in accessibility is strictly due to altered translational positions of the nucleosomes or to alteration of DNA contacts with the histone octamer. In this study, we clearly demonstrate that the process of nucleosome sliding by ISW2 itself does not increase accessibility of nucleosomal DNA to restriction endonucleases. This result is consistent with the maintenance of the canonical structure of the slid nucleosome shown by histone-DNA mapping and indicates the absence of transiently accessible intermediates, such as looped DNA conformations during ISW2 remodeling and sliding.

The transcription activator Gal4-VP16 bound to linker DNA did not block nucleosome sliding by ISW2, but instead, Gal4-VP16 was displaced by ISW2. The binding of Gal4-VP16 to nearly all of the linker DNA in the183-bp nucleosome did not prevent the nucleosome from sliding the edge of the nucleosome midway through the Gal4 site. Nucleosomes with longer linker DNA were slid completely over the Gal4 site, placing the Gal4 site close to the dyad axis. Sliding of the nucleosome completely over the Gal4 site promoted the displacement of Gal4-VP16 from DNA, which was not observed when sliding was only to the edge

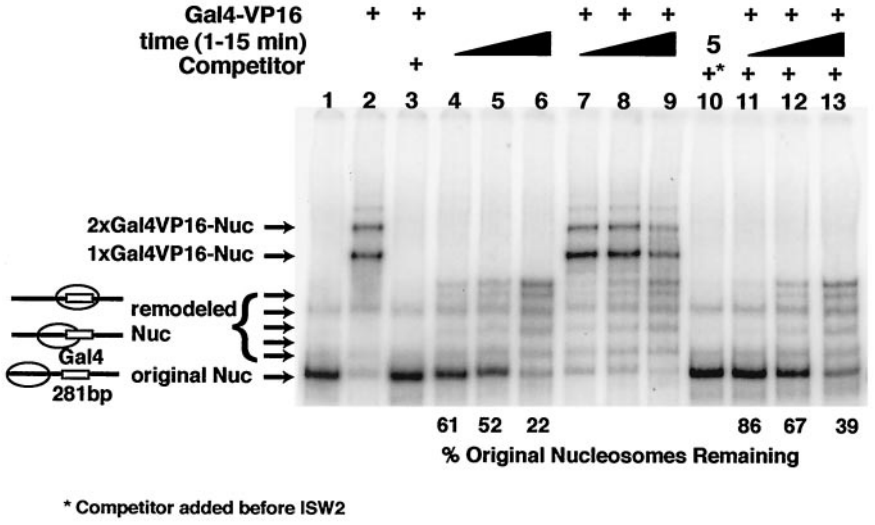

FIG. 5. Gal4-VP16 does not block nucleosome sliding by ISW2. Gal4VP16 was prebound to nucleosomes for 30 min at 30°C in reaction mixtures containing 300 μM ATP, 4.6 pmol of Gal4-VP16, and 3.4 pmol of nucleosomes, and remodeling was started by addition of 0.2 pmol of ISW2 for 1 to 15 min (lanes 4 to 13). After remodeling, Gal4-VP16 was competed with 25 pmol of a short DNA fragment containing single Gal4 binding site for 5 min at 30°C (lanes 3 and 10 to 13). To stop remodeling during competition, the reaction mixture was supplemented with 10 mM γ-S-ATP and 3 μg of salmon sperm DNA. The reactions were analyzed by gel shift on 5% polyacrylamide native PAGE (acrylamide/bisacrylamide ratio, 60/1) gel containing 0.2× TBE at 4°C. In lane 10, the salmon sperm DNA and γ-S-ATP were added before the addition of ISW2.

of the nucleosome. The putative interaction of ISW2 with linker DNA alone was not sufficient to remove Gal4-VP16, but instead seems potentially able to simultaneously interact with linker DNA while bound by Gal4-VP16. The displacement of Gal4-VP16 is likely due to direct interactions with ISW2, but to be caused by its binding site becoming more obstructed due to its location within the nucleosome. These results establish that ISW2 is capable of counteracting transcription activators by placing them within a nucleosome-bound region and displacing them from their cognate sites in order to form a repressive state. In contrast, SWI/SNF remodeling disrupts the nucleosome, enhances the binding of transcription factors, and leads to displacement of the histone octamer from DNA (10, 37, 50). These findings are different from those recently obtained with the NURF complex, in which nucleosomes could not be slid into a Gal4-VP16-bound region (25). The apparent difference may be due to variation in the number of Gal4 binding sites in the linker DNA (one versus five) or may reflect some inherent difference between the two ISWI complexes (ISW2 versus NURF).

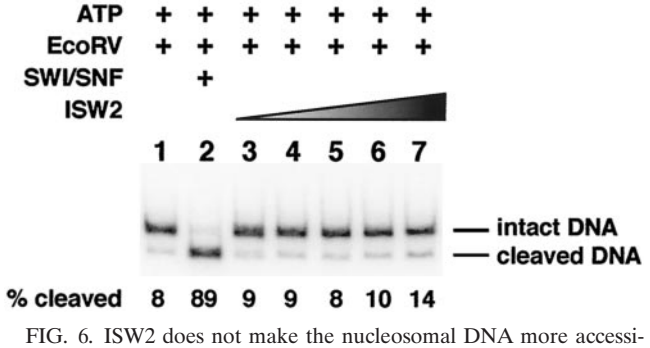

FIG. 6. ISW2 does not make the nucleosomal DNA more accessible to the restriction endonuclease *Eco*RV. Sucrose gradient-purified nucleosomes (10 nM) were subjected to cleavage with *Eco*RV (200 U) in the absence (lane 1) or presence of various amounts of ISW2 (2 to 150 nM, lanes 3 to 7) or SWI/SNF (50 nM, lane 2) and ATP (800 μm) for 40 min at 30°C. Free DNA was digested to completion under those conditions in less than 0.5 min (data not shown). After deproteinizing, the cleaved DNA was resolved from the intact DNA on a 4% native polyacrylamide gel, and the signal in the bands was quantified by phosphorimaging.

Although both SWI/SNF and ISW2 mobilize nucleosomes, our results presented here with ISW2 and others obtained with SWI/SNF and RSC suggest that these complexes do not slide nucleosomes in a similar manner (3, 31). In contrast to ISW2, SWI/SNF, and RSC have been shown to slide nucleosomes up to 50 bp off the ends of the DNA in a mononucleosome, consistent with the reduction in the DNA mass of the remodeled nucleosome observed by electron microscopy (results not shown). The DNA in the nucleosome remodeled by SWI/SNF is likely not to maintain its canonical path on the histone octamer surface, as suggested by changes in DNA supercoiling and nuclease sensitivity (2, 18, 19, 26, 36). These observations are consistent with the restriction cutting assay showing that SWI/SNF, unlike ISW2, is disruptive to the nucleosome structure. Although sliding by ISW2 changes the translational position, it apparently causes no other structural changes that would make the DNA more accessible, and thus these data are consistent with this chromatin remodeling complex being exclusively involved in transcriptional repression.

ACKNOWLEDGMENTS

This work was supported by Public Health Service grant GM48413 from the National Institute of General Medical Sciences and by American Cancer Society grant RPG-99-199-01-GMC.

We also thank K. Luger and T. Richmond for their histone overexpression plasmids.

REFERENCES

1. **Aalfs, J. D., G. J. Narlikar, and R. E. Kingston.** 2001. Functional differences between the human ATP-dependent nucleosome remodeling proteins BRG1 and SNF2H. J. Biol. Chem. **276:**34270–34278.
2. **Aoyagi, S., G. Narlikar, C. Zheng, S. Sif, R. E. Kingston, and J. J. Hayes.** 2002. Nucleosome remodeling by the human SWI/SNF complex requires

transient global disruption of histone-DNA interactions. Mol. Cell. Biol. **22:**3653–3662.
3. **Bazett-Jones, D. P., J. Côté, C. C. Landel, C. L. Peterson, and J. L. Workman.** 1999. The SWI/SNF complex creates loop domains in DNA and polynucleosome arrays and can disrupt DNA-histone contacts within these domains. Mol. Cell. Biol. **19:**1470–1478.
4. **Bonner, W. M., M. H. West, and J. D. Stedman.** 1980. Two-dimensional gel analysis of histones in acid extracts of nuclei, cells, and tissues. Eur. J. Biochem. **109:**17–23.
5. **Boyer, L. A., C. Logie, E. Bonte, P. B. Becker, P. A. Wade, A. P. Wolffe, C. Wu, A. N. Imbalzano, and C. L. Peterson.** 2000. Functional delineation of three groups of the ATP-dependent family of chromatin remodeling enzymes. J. Biol. Chem. **275:**18864–18870.
6. **Brehm, A., G. Langst, J. Kehle, C. R. Clapier, A. Imhof, A. Eberharter, J. Muller, and P. B. Becker.** 2000. dMi-2 and ISWI chromatin remodelling factors have distinct nucleosome binding and mobilization properties. EMBO J. **19:**4332–4341.
7. **Chen, Y., and R. H. Ebright.** 1993. Phenyl-azide-mediated photocrosslinking analysis of Cro-DNA interaction. J. Mol. Biol **230:**453–460.
8. **Clapier, C. R., G. Langst, D. F. V. Corona, P. B. Becker, and K. P. Nightingale.** 2001. Critical role for the histone H4 N terminus in nucleosome remodeling by ISWI. Mol. Cell. Biol. **21:**875–883.
9. **Corona, D. F., A. Eberharter, A. Budde, R. Deuring, S. Ferrari, P. Varga-Weisz, M. Wilm, J. Tamkun, and P. B. Becker.** 2000. Two histone fold proteins, CHRAC-14 and CHRAC-16, are developmentally regulated subunits of chromatin accessibility complex (CHRAC). EMBO J. **19:**3049–3059.
10. **Cote, J., C. L. Peterson, and J. L. Workman.** 1998. Perturbation of nucleosome core structure by the SWI/SNF complex persists after its detachment, enhancing subsequent transcription factor binding. Proc. Natl. Acad. Sci. USA **95:**4947–4952.
11. **Deuring, R., L. Fanti, J. A. Armstrong, M. Sarte, O. Papoulas, M. Prestel, G. Daubresse, M. Verardo, S. L. Moseley, M. Berloco, T. Tsukiyama, C. Wu, S. Pimpinelli, and J. W. Tamkun.** 2000. The ISWI chromatin-remodeling protein is required for gene expression and the maintenance of higher order chromatin structure in vivo. Mol. Cell **5:**355–365.
12. **Eisen, J. A., K. S. Sweder, and P. C. Hanawalt.** 1995. Evolution of the SNF2 family of proteins: subfamilies with distinct sequences and functions. Nucleic Acids Res. **23:**2715–2723.
13. **Fazzio, T. G., C. Kooperberg, J. P. Goldmark, C. Neal, R. Basom, J. Delrow, and T. Tsukiyama.** 2001. Widespread collaboration of Isw2 and Sin3-Rpd3 chromatin remodeling complexes in transcriptional repression. Mol. Cell. Biol. **21:**6450–6460.
14. **Flaus, A., K. Luger, S. Tan, and T. J. Richmond.** 1996. Mapping nucleosome position at single base-pair resolution by using site-directed hydroxyl radicals. Proc. Natl. Acad. Sci. USA **93:**1370–1375.
15. **Georgel, P. T., T. Tsukiyama, and C. Wu.** 1997. Role of histone tails in nucleosome remodeling by *Drosophila* NURF. EMBO J. **16:**4717–4726.
16. **Goldmark, J. P., T. G. Fazzio, P. W. Estep, G. M. Church, and T. Tsukiyama.** 2000. The Isw2 chromatin remodeling complex represses early meiotic genes upon recruitment by Ume6p. Cell **103:**423–433.
17. **Guschin, D., P. A. Wade, N. Kikyo, and A. P. Wolffe.** 2000. ATP-dependent histone octamer mobilization and histone deacetylation mediated by the Mi-2 chromatin remodeling complex. Biochemistry **39:**5238–5245.
18. **Guyon, J. R., G. J. Narlikar, S. Sif, and R. E. Kingston.** 1999. Stable remodeling of tailless nucleosomes by the human SWI-SNF complex. Mol. Cell. Biol. **19:**2088–2097.
19. **Guyon, J. R., G. J. Narlikar, E. K. Sullivan, and R. E. Kingston.** 2001. Stability of a human SWI-SNF remodeled nucleosomal array. Mol. Cell. Biol. **21:**1132–1144.
20. **Hamiche, A., R. Sandaltzopoulos, D. A. Gdula, and C. Wu.** 1999. ATP-dependent histone octamer sliding mediated by the chromatin remodeling complex NURF. Cell **97:**833–842.
21. **Havas, K., A. Flaus, M. Phelan, R. Kingston, P. A. Wade, D. M. Lilley, and T. Owen-Hughes.** 2000. Generation of superhelical torsion by ATP-dependent chromatin remodeling activities. Cell **103:**1133–1142.
22. **Ito, T., M. Bulger, M. J. Pazin, R. Kobayashi, and J. T. Kadonaga.** 1997. ACF, an ISWI-containing and ATP-utilizing chromatin assembly and remodeling factor. Cell **90:**145–155.
23. **Ito, T., M. E. Levenstein, D. V. Fyodorov, A. K. Kutach, R. Kobayashi, and J. T. Kadonaga.** 1999. ACF consists of two subunits, Acf1 and ISWI, that function cooperatively in the ATP-dependent catalysis of chromatin assembly. Genes Dev. **13:**1529–1539.
24. **Juan, L. J., R. T. Utley, M. Vignali, L. Bohm, and J. L. Workman.** 1997. H1-mediated repression of transcription factor binding to a stably positioned nucleosome. J. Biol. Chem. **272:**3635–3640.
25. **Kang, J. G., A. Hamiche, and C. Wu.** 2002. GAL4 directs nucleosome sliding induced by NURF. EMBO J. **21:**1406–1413.
26. **Kingston, R. E., and G. J. Narlikar.** 1999. ATP-dependent remodeling and acetylation as regulators of chromatin fluidity. Genes Dev. **13:**2339–2352.
27. **Langst, G., and P. B. Becker.** 2001. ISWI induces nucleosome sliding on nicked DNA. Mol. Cell **8:**1085–1092.
28. **Langst, G., and P. B. Becker.** 2001. Nucleosome mobilization and positioning by ISWI-containing chromatin-remodeling factors. J. Cell Sci. **114:**2561–2568.
29. **Langst, G., E. J. Bonte, D. F. Corona, and P. B. Becker.** 1999. Nucleosome movement by CHRAC and ISWI without disruption or trans-displacement of the histone octamer. Cell **97:**843–852.
30. **Lee, K. M., and J. J. Hayes.** 1997. The N-terminal tail of histone H2A binds to two distinct sites within the nucleosome core. Proc. Natl. Acad. Sci. USA **94:**8959–8964.
31. **Lorch, Y., M. Zhang, and R. D. Kornberg.** 2001. RSC unravels the nucleosome. Mol. Cell **7:**89–95.
32. **Lowary, P. T., and J. Widom.** 1998. New DNA sequence rules for high affinity binding to histone octamer and sequence-directed nucleosome positioning. J. Mol. Biol. **276:**19–42.
33. **Luger, K., A. W. Mader, R. K. Richmond, D. F. Sargent, and T. J. Richmond.** 1997. Crystal structure of the nucleosome core particle at 2.8 A resolution. Nature **389:**251–260.
34. **Luger, K., T. J. Rechsteiner, and T. J. Richmond.** 1999. Expression and purification of recombinant histones and nucleosome reconstitution. Methods Mol. Biol. **119:**1–16.
35. **Luger, K., T. J. Rechsteiner, and T. J. Richmond.** 1999. Preparation of nucleosome core particle from recombinant histones. Methods Enzymol. **304:**3–19.
36. **Narlikar, G. J., M. L. Phelan, and R. E. Kingston.** 2001. Generation and interconversion of multiple distinct nucleosomal states as a mechanism for catalyzing chromatin fluidity. Mol. Cell **8:**1219–1230.
37. **Owen-Hughes, T., R. T. Utley, J. Cote, C. L. Peterson, and J. L. Workman.** 1996. Persistent site-specific remodeling of a nucleosome array by transient action of the SWI/SNF complex. Science **273:**513–516.
38. **Pendergrast, P. S., Y. Chen, Y. W. Ebright, and R. H. Ebright.** 1992. Determination of the orientation of a DNA binding motif in a protein-DNA complex by photocrosslinking. Proc. Natl. Acad. Sci. USA **89:**10287–10291.
39. **Peterson, C. L.** 1996. Multiple SWItches to turn on chromatin? Curr. Opin. Genet. Dev. **6:**171–175.
40. **Pollard, K. J., and C. L. Peterson.** 1997. Role for *ADA/GCN5* products in antagonizing chromatin-mediated transcriptional repression. Mol. Cell. Biol. **17:**6212–6222.
41. **Sengupta, S. M., J. Persinger, B. Bartholomew, and C. L. Peterson.** 1999. Use of DNA photoaffinity labeling to study nucleosome remodeling by SWI/SNF. Methods **19:**434–446.
42. **Shen, F., S. J. Triezenberg, P. Hensley, D. Porter, and J. R. Knutson.** 1996. Critical amino acids in the transcriptional activation domain of the herpesvirus protein VP16 are solvent-exposed in highly mobile protein segments. An intrinsic fluorescence study. J. Biol. Chem. **271:**4819–4826.
43. **Shen, X., G. Mizuguchi, A. Hamiche, and C. Wu.** 2000. A chromatin remodelling complex involved in transcription and DNA processing. Nature **406:**541–544.
44. **Sudarsanam, P., and F. Winston.** 2000. The Swi/Snf family nucleosome-remodeling complexes and transcriptional control. Trends Genet. **16:**345–351.
45. **Tantin, D., T. Chi, R. Hori, S. Pyo, and M. Carey.** 1996. Biochemical mechanism of transcriptional activation by GAL4-VP16. Methods Enzymol. **274:**133–149.
46. **Tate, J. J., J. Persinger, and B. Bartholomew.** 1998. Survey of four different photoreactive moieties for DNA photoaffinity labeling of yeast RNA polymerase III transcription complexes. Nucleic Acids Res. **26:**1421–1426.
47. **Tsukiyama, T., C. Daniel, J. Tamkun, and C. Wu.** 1995. ISWI, a member of the SWI2/SNF2 ATPase family, encodes the 140 kDa subunit of the nucleosome remodeling factor. Cell **83:**1021–1026.
48. **Tsukiyama, T., J. Palmer, C. C. Landel, J. Shiloach, and C. Wu.** 1999. Characterization of the imitation switch subfamily of ATP-dependent chromatin-remodeling factors in *Saccharomyces cerevisiae*. Genes Dev. **13:**686–697.
49. **Tsukiyama, T., and C. Wu.** 1995. Purification and properties of an ATP-dependent nucleosome remodeling factor. Cell **83:**1011–1020.
50. **Utley, R. T., J. Cote, T. Owen-Hughes, and J. L. Workman.** 1997. SWI/SNF stimulates the formation of disparate activator-nucleosome complexes but is partially redundant with cooperative binding. J. Biol. Chem. **272:**12642–12649.
51. **Varga-Weisz, P.** 2001. ATP-dependent chromatin remodeling factors: nucleosome shufflers with many missions. Oncogene **20:**3076–3085.
52. **Varga-Weisz, P. D., M. Wilm, E. Bonte, K. Dumas, M. Mann, and P. B. Becker.** 1997. Chromatin-remodelling factor CHRAC contains the ATPases ISWI and topoisomerase II. Nature **388:**598–602.
53. **Vignali, M., A. H. Hassan, K. E. Neely, and J. L. Workman.** 2000. ATP-dependent chromatin-remodeling complexes. Mol. Cell. Biol. **20:**1899–1910.
54. **Wolffe, A. P., G. Almouzni, K. Ura, D. Pruss, and J. J. Hayes.** 1993. Transcription factor access to DNA in the nucleosome. Cold Spring Harbor Symp. Quant. Biol. **58:**225–235.
55. **Woodage, T., M. A. Basrai, A. D. Baxevanis, P. Hieter, and F. S. Collins.** 1997. Characterization of the CHD family of proteins. Proc. Natl. Acad. Sci. USA **94:**11472–11477.
56. **Wu, J., and M. Grunstein.** 2000. 25 years after the nucleosome model: chromatin modifications. Trends Biochem. Sci. **25:**619–623.
57. **Zhang, Y., and D. Reinberg.** 2001. Transcription regulation by histone methylation: interplay between different covalent modifications of the core histone tails. Genes Dev. **15:**2343–2360.